Available online at www.sciencedirect.com
ScienceDirect
Journal of Sound and Vibration 318 (2008) 247–266
JOURNAL OF SOUND AND VIBRATION
www.elsevier.com/locate/jsvi

Vibration analysis of doubly asymmetric, three-dimensional structures comprising wall and frame assemblies with variable cross-section

B. Rafezy[a], W.P. Howson[b,*]

[a]*Sahand University of Technology, P.O. Box 51335/1996, Tabriz, Iran*
[b]*Cardiff School of Engineering, Cardiff University, The Parade, Cardiff CF24 3AA, UK*

Received 3 October 2006; received in revised form 12 April 2008; accepted 15 April 2008
Handling Editor: A.V. Metrikine
Available online 12 June 2008

Abstract

A global analysis approach to modelling doubly asymmetric, three-dimensional, multi-bay, multi-storey, wall–frame structures is presented in a form that enables the lower numbered natural frequencies to be determined approximately with the certain knowledge that none have been missed. It is assumed that the primary walls and frames of the original structure run in two orthogonal directions and that their properties may vary in a step-wise fashion at one or more storey levels. The structure therefore divides naturally into uniform segments between changes of section properties. A typical segment is then replaced by an equivalent shear–flexure–torsion coupled beam whose governing differential equations are formulated using a continuum approach and posed in the form of a dynamic member stiffness matrix. The original structure can then be re-modelled as a sophisticated stepped cantilever in the usual way. Since the mass of each segment is assumed to be uniformly distributed, it is necessary to solve a transcendental eigenvalue problem, which is accomplished using the Wittrick–Williams algorithm. A parametric study on a series of wall–frame structures of varying height with different plan configurations is given to compare the accuracy of the current approach with datum results from fully converged finite element analyses.

1. Introduction

There is evidence to suggest that it can be time consuming, unproductive and indeed unnecessary to develop detailed structural models in many areas of application, such as the early stages of a design process, when the concept may be evolving rapidly, or when it is necessary to check solutions developed elsewhere [1]. A compelling alternative in such circumstances is to use a global (holistic) model, developed especially for the type of structure under consideration, which models only the dominant characteristics of the structure. This theme is developed throughout the paper and yields an accurate model that utilises sophisticated theory to describe the motion of a shear–flexure–torsion coupled beam. The theory is presented in the form of a dynamic

*Corresponding author. Tel.: +44 2920 874263; fax: +44 2920 874597.
E-mail address: howson@cf.ac.uk (W.P. Howson).

0022-460X/$ - see front matter © 2008 Elsevier Ltd. All rights reserved.
doi:10.1016/j.jsv.2008.04.018

stiffness matrix for an exact beam finite element that can be used to model the original structure as a series of contiguous elements. The rules for reducing the original structure to the simpler stepped cantilever are given, but can be substantially influenced by the engineer's experience and judgement and as such makes its implementation an inclusive process, where the engineer is at the heart of the solution procedure in a way that can sometimes be lost when using fully automated, general software. Once the equivalent cantilever is established, it can be solved exactly so that no additional accuracy is lost in solution. The following review of related work serves to highlight the growing popularity of such techniques.

Approximate methods have recently been developed that can deal with the vibration of asymmetric three-dimensional structures, in which the translational and torsional modes of vibration are coupled. Kuang and Ng [2,3] considered the problem of doubly asymmetric, proportional structures in which the motion is dominated by shear walls. For the analysis, the structure is replaced by an equivalent uniform cantilever whose deformation is coupled in flexure and warping torsion. The same authors extended this concept to the case of wall–frame structures by allowing for bending and shear. In this case however, the wall and frame systems are independently proportional, but result in a non-proportional structural form [4]. In a recent publication they have extended their work to tall building structures comprising frames, walls, structural cores and coupled walls [5]. As in their previous work, they have replaced the structure with a uniform cantilever, derived the governing differential equation for free vibration and then solved the corresponding eigenvalue problem using a generalised method based on the Galerkin technique. Wall–frame structures have also been addressed by Wang et al. [6], who used an equivalent eccentricity technique that is appropriate for non-proportional structures. However, the analysis is limited to finding the first two coupled natural frequencies of uniform structures with singly asymmetric plan form.

Hand methods have also received considerable attention and are particularly suitable for check calculations. In recent papers by Zalka [7,8], such a method is presented that can deal with the three-dimensional frequency analysis of buildings braced by frameworks, coupled shear-walls and cores.

In a relatively recent publication, Potzta and Kollar [9] replaced the original structure by an equivalent sandwich beam that can model both slender and wide structures consisting of frames, trusses and coupled shear walls. In a subsequent paper, an alternative approach is adopted in which the natural frequencies of the replacement beam are solved approximately. This, together with other simplifying assumptions, leads to simple formulae for determining the required natural frequencies [10]. A useful tabulated summary of related work by the following authors [7,11–18] is also included.

The most recent contribution has been made by Rafezy et al. [19] who presented a simple, accurate model for the calculation of natural frequencies of asymmetric, three-dimensional frame structures whose properties may vary through the height of the structure in a stepwise fashion at one or more storey levels. Their stiffness formulation enables the structure to be modelled as a stepped shear-torsion cantilever which yields the lower natural frequencies for medium to tall structures relatively accurately.

The methods developed in the references above offer solutions of varying accuracy depending on the assumptions employed. Surprisingly, apart from the latter paper by Rafezy et al. [19], none of them allows for step changes of properties along the height of the structure, despite the fact that this is almost inevitably the case in practical building structures of reasonable height. This study therefore seeks to extend the concept of that paper to wall–frame structures.

2. Problem statement

The class of building structure considered herein comprises two sets of orthogonal plane frames that are additionally stiffened by shear walls running in the same orthogonal directions. It is assumed that each frame is of normal proportion so that its dominant response can be modelled using its in-plane shearing characteristics, while each shear wall is assumed to be modelled satisfactorily by its in-plane bending characteristics.

Consider first a typical frame. The in-plane sway motion of such a component is well known to be a synthesis of three characteristic modes of vibration [7] corresponding to (a) full height bending of the individual columns (usually referred to as local bending of the columns); (b) global bending of the structure with significant axial deformation of the columns; and (c) inter-storey shear deformation. These are shown in

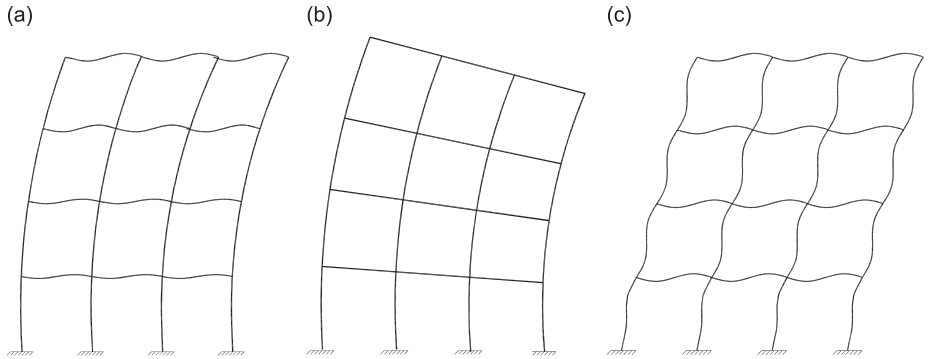

Fig. 1. Components of frame deformation: (a) full height bending of the individual columns (usually referred to as local bending of the columns); (b) global bending of the structure with significant axial deformation of the columns; and (c) inter-storey shear deformation.

Fig. 1. The theoretical model proposed deals accurately with inter-storey shear, but lacks any stiffness contribution stemming from local bending of the columns. The proposed model is therefore more flexible than the original structure in those areas where local bending is important and hence will underestimate the natural frequencies. On the other hand, the columns are assumed to be inextensible and the model will therefore overestimate those frequencies that are significantly influenced by global bending. Since local bending is most prominent in buildings with low slenderness and global bending is most prominent in buildings with relatively high slenderness, there is likely to be a useful range of buildings for which the model yields acceptable results. The model validity range has been discussed previously by Rafezy et al. [19] for the corresponding problem of 3D building structures with doubly asymmetric floor plans, but constructed solely from a series of orthogonal plane frames.

Turning now to the wall systems, it has already been assumed that they deflect predominantly in a flexural configuration. It is now further assumed that the aspect ratio of the walls for in-plane bending in tall buildings is such that they can be modelled realistically using Bernoulli–Euler beam theory, although the effects of shear deformation and rotary inertia could be included straightforwardly and would lead to marginally lower natural frequencies being predicted at the expense of clarity in the theoretical development [24].

More generally, the model also allows for the possibility of a doubly asymmetric floor plan, with the result that the coupling between lateral and torsional motion can become significant and sometimes even critical in tall buildings. This is further complicated when restraint at foundation level causes warping deformations in the walls. This warping-restrained torsion is usually referred to as Vlasov's torsion and can lead to longitudinal stresses in the walls that are sometimes greater than longitudinal stresses due to overall bending of the structure. In the present study the warping rigidity of the walls is taken into account, but the St. Venant torsional component of the walls, which is dependent on circular shear flows within individual wall elements, is small in comparison and is therefore ignored.

The underlying approach adopted with the model is to dissect the original building structure into segments, by cutting through the structure horizontally at those storey levels corresponding to changes in storey properties. Thus the storeys contained within a segment between any two adjacent cut planes are identical. A typical segment is then considered in isolation. Initially, a primary frame in one direction is replaced by a substitute shear beam and a primary wall by a substitute flexural beam. In the case of the shear beam, its mass/unit length is equal to the total mass of the segmented portion of the original frame divided by the segment length. Its stiffness is defined by an equivalent shear stiffness calculated from the properties of the original beams and columns comprising the segment [1,7]. The uniformly distributed mass of the substitute flexural beam is determined similarly from the appropriate segment of the original wall, while its stiffness is merely the corresponding flexural stiffness of the wall. It should be noted that the shear beam has the unusual property of allowing for shearing deformation, but not bending deformation, while the flexural beam allows only for bending deformation. In turn, each frame and wall running in the same direction are replaced by their own substitute beams and the effect of all these beams is summed to model the effect of the original structure. This leads directly to the differential equation governing the motion of the segment in the chosen direction. The

same procedure is then adopted for those frames and walls running in the orthogonal direction. Once both equations are available, it requires little effort to write down the substitute expressions for the coupled torsional motion. The three equations thus formed are subsequently solved exactly and posed in dynamic stiffness form. The resulting coupled shear–flexure–torsion beam element can then be used to reconstitute the original structure by assembling the dynamic stiffness matrices for the individual segments in the usual manner.

It is clear from the element formulation that the final model has a transcendental dependence upon the frequency parameter. The required natural frequencies are therefore determined by solving the model using an exact technique, based on the Wittrick–Williams algorithm, that can be arrested after achieving any desired accuracy and which also ensures that no natural frequencies can be missed.

3. Theory

Fig. 2 shows the hypothetical layout of a typical floor plan of an asymmetric, three-dimensional wall–frame structure, in which the plane frames and walls run in two orthogonal directions. The shear centre of the frames, $S(x_s,y_s)$, at each floor level is assumed to lie on a vertical line, the shear rigidity axis, which runs through the height of the structure. This condition is automatically satisfied when the frames running parallel to the x-axis are all proportional, i.e. their stiffness matrices can be scaled linearly from that of an arbitrary frame, and likewise for frames running parallel to the y-axis, although the arbitrary frame does not have to be the same in both directions. The flexure centre of the walls and the corresponding flexural rigidity axis are defined by analogous arguments. Furthermore, for convenience, the origin of the coordinate system is positioned at the flexure centre, O, with the x,u and y,v axes running parallel to the orthogonal planes containing the walls and frames. The z-axis then runs vertically from the base of the building and coincides with the flexural rigidity axis. Finally, it is assumed that the floor system is rigid in its plane and that the centre of mass at each level, $C(x_c,y_c)$, again lies on a vertical line, the mass axis, which runs through the height of the structure. When the rigidity and mass axes of a structure do not coincide, the lateral and torsional motion of the building will always be coupled in one or more planes.

During vibration, the displacement of the shear and mass centres of a typical floor, (u_s,v_s) and (u_c,v_c), respectively, at any time t in the x–y plane can be determined using Ref. [19] as

$$u_s(z,t) = u(z,t) - y_s\varphi(z,t) \quad \text{and} \quad v_s(z,t) = v(z,t) + x_s\varphi(z,t) \tag{1a,b}$$

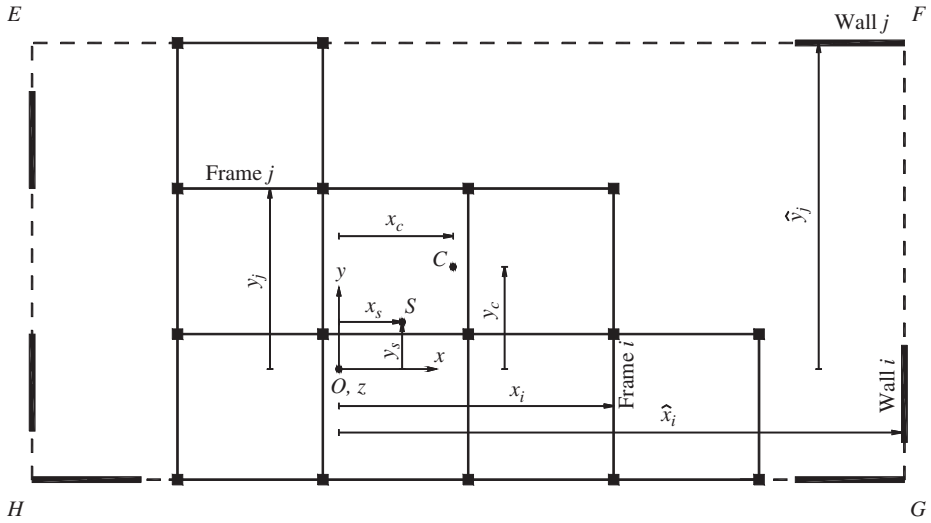

Fig. 2. Typical floor plan of an asymmetric three-dimensional wall–frame structure. O, S and C denote the locations of the flexure, shear and mass centres, respectively. The floor system $EFGH$ is considered to be rigid in its plane.

$$u_c(z,t) = u(z,t) - y_c\varphi(z,t) \quad \text{and} \quad v_c(z,t) = v(z,t) + x_c\varphi(z,t) \tag{1c,d}$$

where $\varphi(z,t)$ is the in-plane rotation of the floor about the flexure centre. More generally, it is clear that the displacements of a typical point (x_i, y_i) are given by Eqs. (1a) and (1b) when $s = i$.

The structure is now divided into segments along the z-axis by notionally cutting the structure along horizontal planes at those storey levels corresponding to changes in storey properties. Fig. 4 shows a typical segment formed by cutting the structure through planes $E_kF_kG_kH_k$ and $E_{k+1}F_{k+1}G_{k+1}H_{k+1}$ that correspond to the kth and k+1th changes in storey properties. The number of storeys in any one segment can vary from one, to the total number of storeys in the structure if it is uniform throughout its height. However, in any one segment each storey must have the same properties (Fig. 3).

We now consider a typical segment in isolation and seek to replace each primary frame by a substitute shear beam and each primary wall with a substitute flexural beam that replicates its in-plane motion. We start by considering a typical frame, frame i, that runs parallel to the y–z plane, see Fig. 2. This whole frame is replaced by the single substitute beam, beam i, shown in Fig. 4. This beam is a two-dimensional shear beam of length L and has uniformly distributed mass and shear stiffness. The local mass and shear rigidity axes therefore both coincide with the local z-axis, which can only undergo shear deformation $v_i(z,t)$ in the y direction, where z and t denote distance from the local origin and time, respectively. Likewise, a typical wall, wall i, running parallel to the y–z plane is replaced by the single flexural substitute beam, beam i, shown in Fig. 5. This beam is a two-dimensional flexural beam of length L and has uniformly distributed mass and flexural stiffness. Once more the local mass and flexural rigidity axes coincide with the local z-axis, which this time can only undergo bending deformation $\hat{v}_i(z,t)$ in the y direction.

The equation of motion for a substitute shear beam in the y–z plane is given in Ref. [19] as

$$\frac{\partial}{\partial z}\left(GA_{yi}\frac{\partial v_i(z,t)}{\partial z}\right) = m_{fyi}\frac{\partial^2 v_i(z,t)}{\partial t^2} \tag{2}$$

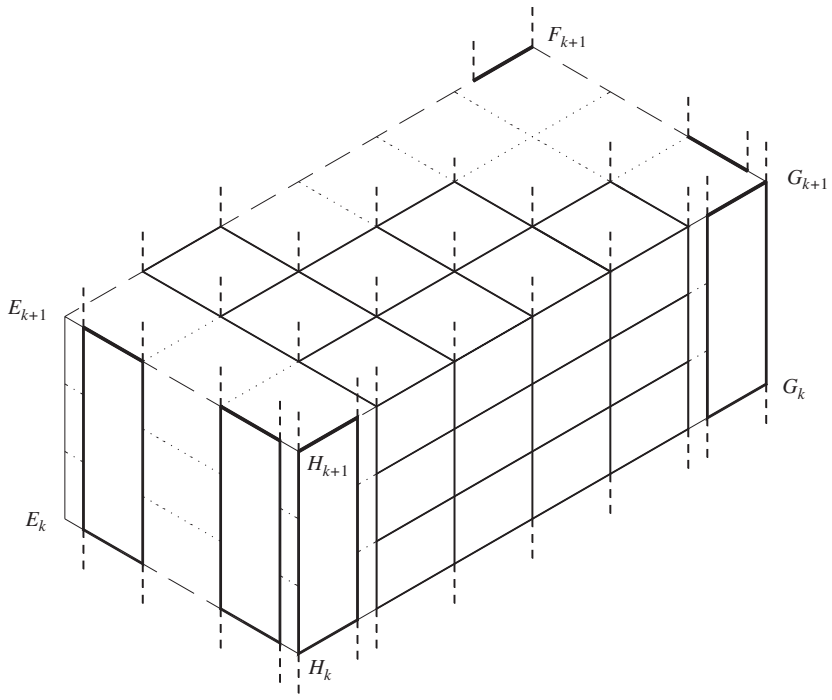

Fig. 3. Typical segment formed by cutting the structure through planes $E_kF_kG_kH_k$ and $E_{k+1}F_{k+1}G_{k+1}H_{k+1}$ that correspond to the kth and $k+1$th changes in storey properties. (Some walls, columns and beam members have been omitted for clarity.)

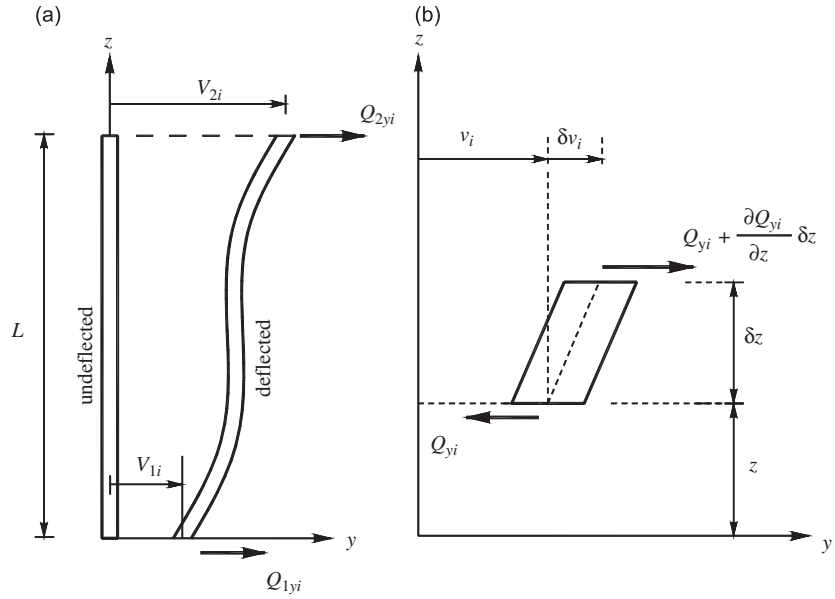

Fig. 4. Coordinate system and positive sign convention for the substitute two-dimensional shear beam in the local y–z plane: (a) member convention and (b) element convention.

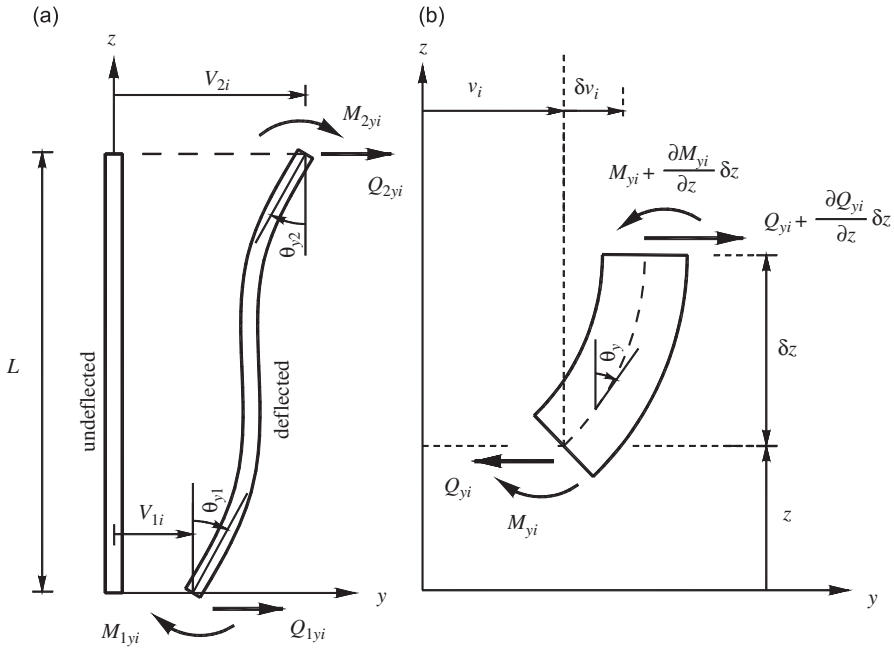

Fig. 5. Coordinate system and positive sign convention for the substitute two-dimensional flexural beam in the local y–z plane: (a) member convention and (b) element convention.

where the constitutive relationship for pure shear is taken as

$$\frac{Q_{fyi}(z,t)}{GA_{yi}} = \frac{\partial v_i(z,t)}{\partial z} \tag{3}$$

In these equations $Q_{fyi}(z,t)$ is the shear force on the element, GA_{yi} is the effective shear rigidity in the y direction [20] and m_{fyi} is the uniformly distributed mass per unit length.

The corresponding equations for a flexural element in the y–z plane are well known and may be written as

$$\frac{\partial}{\partial z}\left(-EI_{yi}\frac{\partial^3 \hat{v}_i(z,t)}{\partial z^3}\right) = m_{wyi}\frac{\partial^2 \hat{v}_i(z,t)}{\partial t^2} \tag{4}$$

and

$$\frac{\partial Q_{wyi}(z,t)}{\partial z} = m_{wyi}\frac{\partial^2 \hat{v}_i(z,t)}{\partial t^2} \tag{5}$$

where $Q_{wyi}(z,t)$ is the shear force on the element, EI_{yi} is the flexural rigidity in the y direction and m_{wyi} is the uniformly distributed mass per unit length.

We now use Eq. (1b), with i in place of c, to eliminate $v_i(z,t)$ and $\hat{v}_i(z,t)$ and assume that GA_{yi} and EI_{yi} are constant over each member. Then, if the replacement procedure is carried out for all the i frames and walls that run parallel to the y–z plane, the dynamic equilibrium for motion in the y–z plane may be written as

$$\sum_{i=1}^{n_{wy}} -EI_{yi}\frac{\partial^4(v(z,t)+\hat{x}_i\varphi(z,t))}{\partial z^4} + \sum_{i=1}^{n_{fy}} GA_{yi}\frac{\partial^2(v(z,t)+x_i\varphi(z,t))}{\partial z^2} - \sum_{i=1}^{n_{wy}} m_{wyi}\frac{\partial^2(v(z,t)+\hat{x}_i\varphi(z,t))}{\partial t^2} - \sum_{i=1}^{n_{fy}} m_{fyi}\frac{\partial^2(v(z,t)+x_i\varphi(z,t))}{\partial t^2} = 0 \tag{6}$$

where n_{fy} and n_{wy} are the number of frames and walls running in the y direction, respectively, and likewise x_i and $\hat{x}_i$ are the distance of frame i and wall i from O.

However, since O is the flexure centre, $\sum_{i=1}^{n_{wy}} EI_{yi}\hat{x}_i = 0$ and Eq. (6) can be simplified to

$$EI_y\frac{\partial^4 v(z,t)}{\partial z^4} - GA_y\frac{\partial^2 v(z,t)}{\partial z^2} - x_s GA_y\frac{\partial^2 \varphi(z,t)}{\partial z^2} + m_y\frac{\partial^2 v(z,t)}{\partial t^2} + x_c m_y\frac{\partial^2 \varphi(z,t)}{\partial t^2} = 0 \tag{7}$$

in which

$$EI_y = \sum_{i=1}^{n_{wy}} EI_{yi} \tag{8a}$$

$$x_s GA_y = \sum_{i=1}^{n_{fy}} x_i GA_{yi} \quad \text{where} \quad GA_y = \sum_{i=1}^{n_{fy}} GA_{yi} \tag{8b}$$

and

$$x_c m_y = \sum_{i=1}^{n_{wy}} \hat{x}_i m_{wyi} + \sum_{i=1}^{n_{fy}} x_i m_{fyi} \quad \text{where} \quad m_y = \sum_{i=1}^{n_{wy}} m_{wyi} + \sum_{i=1}^{n_{fy}} m_{fyi} \tag{8c}$$

Since the total mass of the segment contributes to its vibration, including the mass of the frames and walls running in the x direction and the rigid diaphragms, m_y should be replaced by m, where m is the equivalent distributed mass over the height of the segment. Therefore

$$EI_y\frac{\partial^4 v(z,t)}{\partial z^4} - GA_y\frac{\partial^2 v(z,t)}{\partial z^2} - x_s GA_y\frac{\partial^2 \varphi(z,t)}{\partial z^2} + m\frac{\partial^2 v(z,t)}{\partial t^2} + mx_c\frac{\partial^2 \varphi(z,t)}{\partial t^2} = 0 \tag{9}$$

In an identical fashion, the equation of motion in the x–z plane yields the second governing differential equation as

$$EI_x\frac{\partial^4 u(z,t)}{\partial z^4} - GA_x\frac{\partial^2 u(z,t)}{\partial z^2} + y_s GA_x\frac{\partial^2 \varphi(z,t)}{\partial z^2} + m\frac{\partial^2 u(z,t)}{\partial t^2} - my_c\frac{\partial^2 \varphi(z,t)}{\partial t^2} = 0 \tag{10}$$

in which

$$EI_x = \sum_{j=1}^{n_{wx}} EI_{wxj} \quad \text{and} \quad GA_x = \sum_{j=1}^{n_{fx}} GA_{xj} \tag{11a,b}$$

Finally, it should be noted that the plane frames and walls running parallel to the x–z and y–z planes also provide the torsional stiffness of the building [19]. Thus the required equation for torsion can be developed from a consideration of the torsional equilibrium about O, which yields

$$EI_w\frac{\partial^4\varphi(z,t)}{\partial z^4}-x_sGA_y\frac{\partial^2 v(z,t)}{\partial z^2}+y_sGA_x\frac{\partial^2 u(z,t)}{\partial z^2}-GJ\frac{\partial^2\varphi(z,t)}{\partial z^2}+m_yx_c\frac{\partial^2 v(z,t)}{\partial t^2}-m_xy_c\frac{\partial^2 u(z,t)}{\partial t^2}+I_g\frac{\partial^2\varphi(z,t)}{\partial t^2}=0 \tag{12}$$

where

$$EI_w=\sum_{i=1}^{n_{wy}}EI_{yi}\hat{x}_i^2+\sum_{j=1}^{n_{wx}}EI_{xj}\hat{y}_j^2 \tag{13a}$$

$$GJ=\sum_{i=1}^{n_y}GA_{yi}x_i^2+\sum_{j=1}^{n_x}GA_{xj}y_j^2 \tag{13b}$$

$$I_g=\sum_{i=1}^{n_{wy}}m_{wyi}\hat{x}_i^2+\sum_{j=1}^{n_{wx}}m_{wxj}\hat{y}_j^2+\sum_{i=1}^{n_y}m_{fyi}x_i^2+\sum_{j=1}^{n_x}m_{fxj}y_j^2 \tag{13c}$$

where EI_w, GJ and I_g are the torsional rigidity of the walls, the torsional rigidity of the frames and the polar second moment of mass about the flexure centre O, respectively. Comparing Eq. (12) with the theory describing the torsion of members with thin walled cross-sections, EI_w and GJ can be recognised as the warping and Saint-Venant torsional rigidity, respectively.

As before, the total mass of the frames and walls running in the x and y directions, as well as that of the rigid diaphragms, should be taken into account. Thus Eqs. (9), (10) and (12) can finally be rearranged and written in the following form:

$$EI_x\frac{\partial^4 u(z,t)}{\partial z^4}-GA_x\frac{\partial^2 u(z,t)}{\partial z^2}+y_sGA_x\frac{\partial^2\varphi(z,t)}{\partial z^2}+m\frac{\partial^2 u(z,t)}{\partial t^2}-my_c\frac{\partial^2\varphi(z,t)}{\partial t^2}=0 \tag{14a}$$

$$EI_y\frac{\partial^4 v(z,t)}{\partial z^4}-GA_y\frac{\partial^2 v(z,t)}{\partial z^2}-x_sGA_y\frac{\partial^2\varphi(z,t)}{\partial z^2}+m\frac{\partial^2 v(z,t)}{\partial t^2}+mx_c\frac{\partial^2\varphi(z,t)}{\partial t^2}=0 \tag{14b}$$

$$EI_w\frac{\partial^4\varphi(z,t)}{\partial z^4}-GJ\frac{\partial^2\varphi(z,t)}{\partial z^2}+y_sGA_x\frac{\partial^2 u(z,t)}{\partial z^2}-x_sGA_y\frac{\partial^2 v(z,t)}{\partial z^2}-my_c\frac{\partial^2 u(z,t)}{\partial t^2}+mx_c\frac{\partial^2 v(z,t)}{\partial t^2}+mr_m^2\frac{\partial^2\varphi(z,t)}{\partial t^2}=0 \tag{14c}$$

where r_m is the polar mass radius of gyration of the structure about the flexure centre, O. Eqs. (14a–c) are the required differential equations of motion.

4. Eigenvalue problem

Eqs. (14) are now solved and posed in dynamic stiffness form. Although each equation was developed individually from a consideration of the planar shear and flexural beams of Figs. 4 and 5, they now describe the motion of a three-dimensional, shear–flexure–torsion coupled beam whose coordinate system and sign convention are shown in Fig. 6. This substitute beam (exact finite element) will be used to model each segment of the original, asymmetric, three-dimensional wall–frame structure. The whole of the original structure can then be modelled by assembling the substitute beams corresponding to each segment in the usual way.

Eqs. (14) are solved on the assumption of harmonic motion, so that the instantaneous displacements can be written as

$$u(z,t)=U(z)\sin\omega t\quad v(z,t)=V(z)\sin\omega t\quad \varphi(z,t)=\Phi(z)\sin\omega t \tag{15a–c}$$

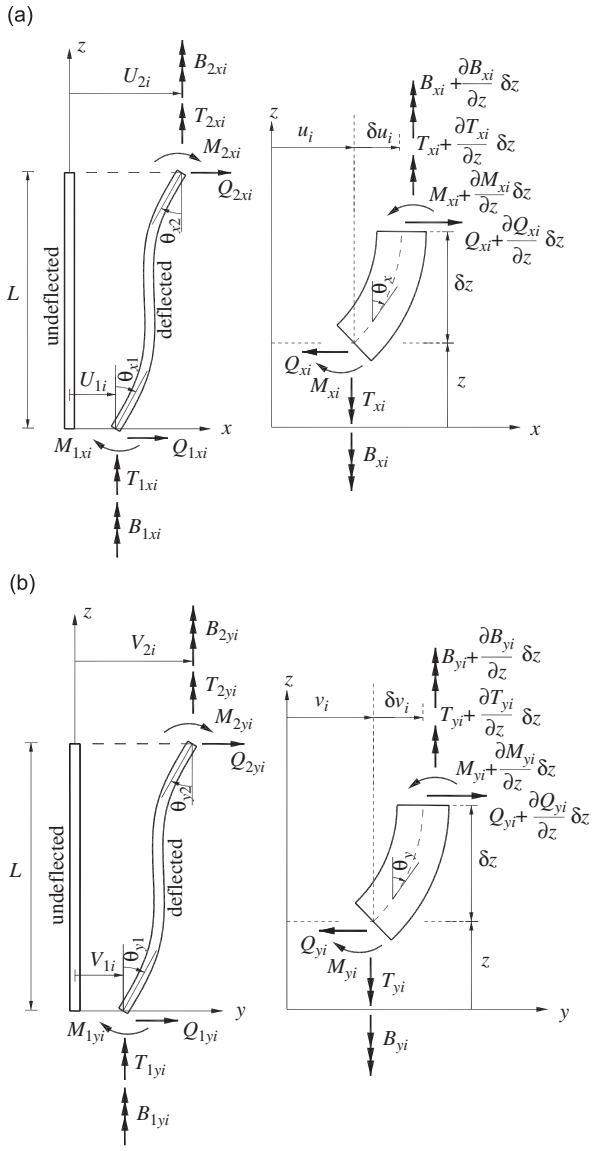

Fig. 6. Coordinate system and positive sign convention for the substitute three-dimensional shear–flexure–torsion beam: (a) member and element convention for the x–z plane, and (b) member and element convention for the y–z plane.

where $U(z)$, $V(z)$ and $\Phi(z)$ are the amplitudes of the sinusoidally varying displacements and ω is the circular frequency.

Substituting Eqs. (19) into Eqs. (18) and re-writing in non-dimensional form gives

$$U''''(\xi) - \alpha_x^2 U''(\xi) + y_s \alpha_x^2 \Phi''(\xi) - \beta_x^2 \omega^2 U(\xi) + y_c \omega^2 \beta_x^2 \Phi(\xi) = 0 \tag{16a}$$

$$V''''(\xi) - \alpha_y^2 V''(\xi) - x_s \alpha_y^2 \Phi''(\xi) - \beta_y^2 \omega^2 V(\xi) - x_c \omega^2 \beta_y^2 \Phi(\xi) = 0 \tag{16b}$$

$$\begin{aligned} &\Phi''''(\xi) - \alpha_\varphi^2 \Phi''(\xi) + y_s \frac{\alpha_x^2}{\gamma_x^2} U''(\xi) - x_s \frac{\alpha_y^2}{\gamma_y^2} V''(\xi) \\ &- \omega^2 \beta_\varphi^2 \Phi(\xi) + y_c \omega^2 \frac{\beta_x^2}{\gamma_x^2} U(\xi) - x_c \omega^2 \frac{\beta_y^2}{\gamma_y^2} V(\xi) = 0 \end{aligned} \tag{16c}$$

where

$$\alpha_x^2 = \frac{GA_x}{EI_x}L^2, \quad \alpha_y^2 = \frac{GA_y}{EI_y}L^2 \quad \text{and} \quad \alpha_\varphi^2 = \frac{GJ}{EI_w}L^2 \tag{17a–c}$$

$$\beta_x^2 = \frac{mL^4}{EI_x}, \quad \beta_y^2 = \frac{mL^4}{EI_y} \quad \text{and} \quad \beta_\varphi^2 = r_m^2\frac{mL^4}{EI_w} \tag{17d–f}$$

$$\gamma_x^2 = \frac{EI_w}{EI_x}, \quad \gamma_y^2 = \frac{EI_w}{EI_y} \quad \text{and} \quad \xi = \frac{z}{L} \tag{17g–i}$$

Eqs. (16) can be re-written in the following matrix form:

$$\mathbf{A}\begin{bmatrix} U(\xi) \\ V(\xi) \\ \Phi(\xi) \end{bmatrix} = \mathbf{0} \tag{18}$$

where

$$\mathbf{A} = \begin{bmatrix} \tau^2 - \alpha_x^2\tau - \omega^2\beta_x^2 & 0 & y_s\alpha_x^2\tau + y_c\omega^2\beta_x^2 \\ 0 & \tau^2 - \alpha_y^2\tau - \omega^2\beta_y^2 & -x_s\alpha_y^2\tau - x_c\omega^2\beta_y^2 \\ y_s\dfrac{\alpha_x^2}{\gamma_x^2}\tau + y_c\omega^2\dfrac{\beta_x^2}{\gamma_x^2} & -x_s\dfrac{\alpha_y^2}{\gamma_y^2}\tau - x_c\omega^2\dfrac{\beta_y^2}{\gamma_y^2} & \tau^2 - \alpha_\varphi^2\tau - \omega^2\beta_\varphi^2 \end{bmatrix} \tag{19}$$

and $D = \mathrm{d}/\mathrm{d}\xi$ and $\tau = D^2$.

Eq. (18) can be combined into one equation by eliminating either U, V or Φ to give the twelfth-order differential equation

$$|\mathbf{A}|W(\xi) = 0 \tag{20}$$

where $W = U$, V or Φ.

The solution of Eq. (20) is found by substituting the trial solution $W(\xi) = \mathrm{e}^{a\xi}$ to yield the characteristic equation

$$|\mathbf{A}|W(\xi) = 0 \tag{21}$$

in which $\tau = a^2$.

Eq. (21) is a sixth order equation in τ and it can be proven that it always has three negative and three positive real roots. Let these six roots be τ_1, τ_2, τ_3, $-\tau_4$, $-\tau_5$ and $-\tau_6$, where τ_j ($j = 1,6$) are all real and positive. Therefore the twelve roots of Eq. (21) can be obtained as

$$\alpha, -\alpha \quad \beta, -\beta \quad \gamma, -\gamma \quad \mathrm{i}\delta, -\mathrm{i}\delta \quad \mathrm{i}\eta, -\mathrm{i}\eta \quad \mathrm{i}\mu, -\mathrm{i}\mu \tag{22a}$$

where

$$\alpha = \sqrt{\tau_1}, \quad \beta = \sqrt{\tau_2}, \quad \gamma = \sqrt{\tau_3}, \quad \delta = \sqrt{\tau_4}, \quad \eta = \sqrt{\tau_5}, \quad \text{and} \quad \mu = \sqrt{\tau_6} \tag{22b}$$

and $\mathrm{i} = \sqrt{-1}$.

It follows that the solution of Eq. (20) is of the form

$$\begin{aligned} W(\xi) = {} & C_1\cosh\alpha\xi + C_2\sinh\alpha\xi + C_3\cosh\beta\xi + C_4\sinh\beta\xi + C_5\cosh\gamma\xi + C_6\sinh\gamma\xi \\ & + C_7\cos\delta\xi + C_8\sin\delta\xi + C_9\cos\eta\xi + C_{10}\sin\eta\xi + C_{11}\cos\mu\xi + C_{12}\sin\mu\xi \end{aligned} \tag{23}$$

Eq. (23) represents the solution for $U(\xi)$, $V(\xi)$ and $\Phi(\xi)$, since they are related via Eq. (20). Hence they can be written individually as

$$\begin{aligned} U(\xi) = {} & C_1^u\cosh\alpha\xi + C_2^u\sinh\alpha\xi + C_3^u\cosh\beta\xi + C_4^u\sinh\beta\xi + C_5^u\cosh\gamma\xi + C_6^u\sinh\gamma\xi \\ & + C_7^u\cos\delta\xi + C_8^u\sin\delta\xi + C_9^u\cos\eta\xi + C_{10}^u\sin\eta\xi + C_{11}^u\cos\mu\xi + C_{12}^u\sin\mu\xi \end{aligned} \tag{24a}$$

$$V(\xi) = C_1^v \cosh \alpha\xi + C_2^v \sinh \alpha\xi + C_3^v \cosh \beta\xi + C_4^v \sinh \beta\xi + C_5^v \cosh \gamma\xi + C_6^v \sinh \gamma\xi + C_7^v \cos \delta\xi + C_8^v \sin \delta\xi + C_9^v \cos \eta\xi + C_{10}^v \sin \eta\xi + C_{11}^v \cos \mu\xi + C_{12}^v \sin \mu\xi \quad (24b)$$

$$\Phi(\xi) = C_1 \cosh \alpha\xi + C_2 \sinh \alpha\xi + C_3 \cosh \beta\xi + C_4 \sinh \beta\xi + C_5 \cosh \gamma\xi + C_6 \sinh \gamma\xi + C_7 \cos \delta\xi + C_8 \sin \delta\xi + C_9 \cos \eta\xi + C_{10} \sin \eta\xi + C_{11} \cos \mu\xi + C_{12} \sin \mu\xi \quad (24c)$$

The relationship between the constants C_j^u, C_j^v and $C_j (j = 1,12)$ also follows from Eq. (20) as

$$C_{2j-1}^u = t_j^u C_{2j-1} \quad \text{and} \quad C_{2j}^u = t_j^u C_{2j} \quad (j = 1,6) \quad (25a,b)$$

$$C_{2j-1}^v = t_j^v C_{2j-1} \quad \text{and} \quad C_{2j}^v = t_j^v C_{2j} \quad (j = 1,6) \quad (25c,d)$$

where

$$t_j^u = \frac{-y_s\alpha_x^2\tau_j - y_c\omega^2\beta_x^2}{\tau_j^2 - \alpha_x^2\tau_j - \omega^2\beta_x^2} \ (j = 1,2,3), \quad t_j^u = \frac{y_s\alpha_x^2\tau_j - y_c\omega^2\beta_x^2}{\tau_j^2 + \alpha_x^2\tau_j - \omega^2\beta_x^2} \ (j = 4,5,6) \quad (26a,b)$$

$$t_j^v = \frac{x_s\alpha_y^2\tau_j + x_c\omega^2\beta_y^2}{\tau_j^2 - \alpha_y^2\tau_j - \omega^2\beta_y^2} \ (j = 1,2,3), \quad t_j^v = \frac{-x_s\alpha_y^2\tau_j + x_c\omega^2\beta_y^2}{\tau_j^2 + \alpha_y^2\tau_j - \omega^2\beta_y^2} \ (j = 4,5,6) \quad (26c,d)$$

Following the sign convention of Figs. 4(a) and (b), expressions for the bending rotations $\theta_x(\xi)$, $\theta_y(\xi)$ and the gradient of the twist $\Phi'(\xi)$ are easily established as

$$\theta_x(\xi) = \frac{1}{L}\frac{dU(\xi)}{d\xi}, \quad \theta_y(\xi) = \frac{1}{L}\frac{dV(\xi)}{d\xi} \quad \text{and} \quad \Phi'(\xi) = \frac{1}{L}\frac{d\Phi(\xi)}{d\xi} \quad (27a-c)$$

The corresponding bending moments $M_x(\xi)$, $M_y(\xi)$ and the bi-moment $B(\xi)$ are likewise easily determined from the appropriate stress/strain relationships as

$$M_x(\xi) = \frac{-EI_x}{L^2}\frac{d^2U(\xi)}{d\xi^2}, \quad M_y(\xi) = \frac{-EI_y}{L^2}\frac{d^2V(\xi)}{d\xi^2} \quad \text{and} \quad B(\xi) = \frac{EI_w}{L^2}\frac{d^2\Phi(\xi)}{d\xi^2} \quad (28a-c)$$

Substituting Eqs. (15) and (17i) into Eq. (14) enables the equations for the lateral shear forces and torsional moment to be written as

$$Q_x(\xi) = \frac{-EI_x}{L^3}\frac{d^3U(\xi)}{d\xi^3} + \frac{GA_x}{L}\left(\frac{dU(\xi)}{d\xi} - y_s\frac{d\Phi(\xi)}{d\xi}\right) \quad (28d)$$

$$Q_y(\xi) = \frac{-EI_y}{L^3}\frac{d^3V(\xi)}{d\xi^3} + \frac{GA_y}{L}\left(\frac{dV(\xi)}{d\xi} + x_s\frac{d\Phi(\xi)}{d\xi}\right) \quad (28e)$$

$$T(\xi) = \frac{-EI_w}{L^3}\frac{d^3\Phi(\xi)}{d\xi^3} + \frac{GJ}{L}\frac{d\Phi(\xi)}{d\xi} - y_s\frac{GA_x}{L}\frac{dU(\xi)}{d\xi} + x_s\frac{GA_y}{L}\frac{dV(\xi)}{d\xi} \quad (28f)$$

The nodal displacements and forces can now be defined in the member coordinate system of Figs. 4(a) and (b), as follows:

$$\text{At} \quad \xi = 0 \quad U = U_1, \quad \theta_x = \theta_{1x}, \quad V = V_1, \quad \theta_y = \theta_{1y}, \quad \Phi = \Phi_1, \quad \Phi' = \Phi'_1 \quad (29a)$$

$$\text{At} \quad \xi = 1 \quad U = U_2, \quad \theta_x = \theta_{2x}, \quad V = V_2, \quad \theta_y = \theta_{2y}, \quad \Phi = \Phi_2, \quad \Phi' = \Phi'_2 \quad (29b)$$

$$\text{At} \quad \xi = 0 \quad Q_x = -Q_{1x}, \quad M_x = M_{1x}, \quad Q_y = -Q_{1y}, \quad M_y = M_{1y}, \quad T = -T_1, \quad B = -B_1 \quad (29c)$$

$$\text{At} \quad \xi = 1 \quad Q_x = Q_{2x}, \quad M_x = -M_{2x}, \quad Q_y = Q_{2y}, \quad M_y = -M_{2y}, \quad T = T_2, \quad B = B_2 \tag{29d}$$

Then the nodal displacements can be determined from Eqs. (10) and (12) as

$$\begin{bmatrix} \mathbf{d}_1 \\ \mathbf{d}_2 \end{bmatrix} = \begin{bmatrix} \mathbf{E}_1 & \mathbf{E}_2 & \mathbf{0} & \mathbf{0} \\ \mathbf{0} & \mathbf{0} & \mathbf{E}_1\mathbf{R}_1 & \mathbf{E}_2\mathbf{R}_2 \\ \mathbf{E}_1\mathbf{C}_h & \mathbf{E}_2\mathbf{C} & \mathbf{E}_1\mathbf{S}_h & \mathbf{E}_2\mathbf{S} \\ \mathbf{E}_1\mathbf{R}_1\mathbf{S}_h & -\mathbf{E}_2\mathbf{R}_2\mathbf{S} & \mathbf{E}_1\mathbf{R}_1\mathbf{C}_h & \mathbf{E}_2\mathbf{R}_2\mathbf{C} \end{bmatrix} \begin{bmatrix} \mathbf{C}_o \\ \mathbf{C}_e \end{bmatrix} \tag{30}$$

where

$$\mathbf{d}_1 = \begin{bmatrix} U_1 \\ V_1 \\ \Phi_1 \\ \theta_{1x} \\ \theta_{1y} \\ \Phi'_1 \end{bmatrix}, \quad \mathbf{d}_2 = \begin{bmatrix} U_2 \\ V_2 \\ \Phi_2 \\ \theta_{2x} \\ \theta_{2y} \\ \Phi'_2 \end{bmatrix}, \quad \mathbf{C}_o = \begin{bmatrix} C_1 \\ C_3 \\ C_5 \\ C_7 \\ C_9 \\ C_{11} \end{bmatrix}, \quad \mathbf{C}_e = \begin{bmatrix} C_2 \\ C_4 \\ C_6 \\ C_8 \\ C_{10} \\ C_{12} \end{bmatrix}, \quad \mathbf{E}_1 = \begin{bmatrix} t_1^u & t_2^u & t_3^u \\ t_1^v & t_2^v & t_3^v \\ 1 & 1 & 1 \end{bmatrix}, \quad \mathbf{E}_2 = \begin{bmatrix} t_4^u & t_5^u & t_6^u \\ t_4^v & t_5^v & t_6^v \\ 1 & 1 & 1 \end{bmatrix}$$

$$\mathbf{R}_1 = \frac{1}{L}\begin{bmatrix} \alpha & 0 & 0 \\ 0 & \beta & 0 \\ 0 & 0 & \gamma \end{bmatrix}, \quad \mathbf{R}_2 = \frac{1}{L}\begin{bmatrix} \delta & 0 & 0 \\ 0 & \eta & 0 \\ 0 & 0 & \mu \end{bmatrix}, \quad \mathbf{C}_h = \begin{bmatrix} \cosh\alpha & 0 & 0 \\ 0 & \cosh\beta & 0 \\ 0 & 0 & \cosh\gamma \end{bmatrix},$$

$$\mathbf{S}_h = \begin{bmatrix} \sinh\alpha & 0 & 0 \\ 0 & \sinh\beta & 0 \\ 0 & 0 & \sinh\gamma \end{bmatrix}, \quad \mathbf{C} = \begin{bmatrix} \cos\delta & 0 & 0 \\ 0 & \cos\eta & 0 \\ 0 & 0 & \cos\mu \end{bmatrix}, \quad \mathbf{S} = \begin{bmatrix} \sin\delta & 0 & 0 \\ 0 & \sin\eta & 0 \\ 0 & 0 & \sin\mu \end{bmatrix} \tag{31}$$

Hence the vector of constants $[\mathbf{C}_o\ \mathbf{C}_e]^{\mathrm{T}}$ can be determined from Eq. (30) as

$$\begin{bmatrix} \mathbf{C}_o \\ \mathbf{C}_e \end{bmatrix} = \begin{bmatrix} \mathbf{E}_1 & \mathbf{E}_2 & \mathbf{0} & \mathbf{0} \\ \mathbf{0} & \mathbf{0} & \mathbf{E}_1\mathbf{R}_1 & \mathbf{E}_2\mathbf{R}_2 \\ \mathbf{E}_1\mathbf{C}_h & \mathbf{E}_2\mathbf{C} & \mathbf{E}_1\mathbf{S}_h & \mathbf{E}_2\mathbf{S} \\ \mathbf{E}_1\mathbf{R}_1\mathbf{S}_h & -\mathbf{E}_2\mathbf{R}_2\mathbf{S} & \mathbf{E}_1\mathbf{R}_1\mathbf{C}_h & \mathbf{E}_2\mathbf{R}_2\mathbf{C} \end{bmatrix}^{-1} \begin{bmatrix} \mathbf{d}_1 \\ \mathbf{d}_2 \end{bmatrix} \tag{32}$$

In similar fashion the vector of nodal forces can be determined from Eqs. (28) and (29) as

$$\begin{bmatrix} \mathbf{p}_1 \\ \mathbf{p}_2 \end{bmatrix} = \begin{bmatrix} \mathbf{0} & \mathbf{0} & \mathbf{Q}_1 & \mathbf{Q}_2 \\ \mathbf{M}_1 & \mathbf{M}_2 & \mathbf{0} & \mathbf{0} \\ -\mathbf{Q}_1\mathbf{S}_h & \mathbf{Q}_2\mathbf{S} & -\mathbf{Q}_1\mathbf{C}_h & -\mathbf{Q}_2\mathbf{C} \\ -\mathbf{M}_1\mathbf{C}_h & -\mathbf{M}_2\mathbf{C} & -\mathbf{M}_1\mathbf{S}_h & -\mathbf{M}_2\mathbf{S} \end{bmatrix} \begin{bmatrix} \mathbf{C}_o \\ \mathbf{C}_e \end{bmatrix} \tag{33}$$

where

$$\mathbf{p}_1 = \begin{bmatrix} Q_{1x} \\ Q_{1y} \\ T_1 \\ M_{1x} \\ M_{1y} \\ B_1 \end{bmatrix}, \quad \mathbf{p}_2 = \begin{bmatrix} Q_{2x} \\ Q_{2y} \\ T_2 \\ M_{2x} \\ M_{2y} \\ B_2 \end{bmatrix}, \tag{34a,b}$$

$$\mathbf{Q}_1=\begin{bmatrix} t_1^u(\alpha^3B_x-\alpha C_x)+y_s\alpha C_x & t_2^u(\beta^3B_x-\beta C_x)+y_s\beta C_x & t_3^u(\gamma^3B_x-\gamma C_x)+y_s\gamma C_x \\ t_1^v(\alpha^3B_y-\alpha C_y)-x_s\alpha C_y & t_2^v(\beta^3B_y-\beta C_y)-x_s\beta C_y & t_3^v(\gamma^3B_y-\gamma C_y)-x_s\gamma C_y \\ t_1^u y_s\alpha C_x-t_1^v x_s\alpha C_y+\alpha^3E_o-\alpha F_o & t_2^u y_s\beta C_x-t_2^v x_s\beta C_y+\beta^3E_o-\beta F_o & t_3^u y_s\gamma C_x-t_3^v x_s\gamma C_y+\gamma^3E_o-\gamma F_o \end{bmatrix}$$

$$\mathbf{Q}_2=\begin{bmatrix} t_4^u(-\delta^3B_x-\delta C_x)+y_s\delta C_x & t_5^u(-\eta^3B_x-\eta C_x)+y_s\eta C_x & t_6^u(-\mu^3B_x-\mu C_x)+y_s\mu C_x \\ t_4^v(-\delta^3B_y-\delta C_y)-x_s\delta C_y & t_5^v(-\eta^3B_y-\eta C_y)-x_s\eta C_y & t_6^v(-\mu^3B_y-\mu C_y)-x_s\mu C_y \\ t_4^u y_s\delta C_x-t_4^v x_s\delta C_y-\delta^3E_o-\delta F_o & t_5^u y_s\eta C_x-t_5^v x_s\eta C_y-\eta^3E_o-\eta F_o & t_6^u y_s\mu C_x-t_6^v x_s\mu C_y-\mu^3E_o-\mu F_o \end{bmatrix}$$

$$\mathbf{M}_1=\begin{bmatrix} -t_1^u(\alpha^2A_x) & -t_2^u(\beta^2A_x) & -t_3^u(\gamma^2A_x) \\ -t_1^v(\alpha^2A_y) & -t_2^v(\beta^2A_y) & -t_3^v(\gamma^2A_y) \\ -\alpha^2D_o & -\beta^2D_o & -\gamma^2D_o \end{bmatrix},\quad \mathbf{M}_2=\begin{bmatrix} t_4^u(\delta^2A_x) & t_5^u(\eta^2A_x) & t_6^u(\mu^2A_x) \\ t_4^v(\delta^2A_y) & t_5^v(\eta^2A_y) & t_6^v(\mu^2A_y) \\ \delta^2D_o & \eta^2D_o & \mu^2D_o \end{bmatrix} \tag{35c – f}$$

and

$$A_x=\frac{EI_x}{L^2},\quad A_y=\frac{EI_y}{L^2},\quad B_x=\frac{EI_x}{L^3},\quad B_y=\frac{EI_y}{L^3} \tag{36a–d}$$

$$C_x=\frac{GA_x}{L},\quad C_y=\frac{GA_y}{L},\quad D_o=\frac{EI_w}{L^2},\quad E_o=\frac{EI_w}{L^3},\quad F_o=\frac{GJ}{L} \tag{36e–i}$$

Thus the required stiffness matrix can be developed by substituting Eq. (32) into Eq. (33) to give

$$\begin{bmatrix}\mathbf{p}_1\\ \mathbf{p}_2\end{bmatrix}=\begin{bmatrix} \mathbf{0} & \mathbf{0} & \mathbf{Q}_1 & \mathbf{Q}_2 \\ \mathbf{M}_1 & \mathbf{M}_2 & \mathbf{0} & \mathbf{0} \\ -\mathbf{Q}_1\mathbf{S}_h & \mathbf{Q}_2\mathbf{S} & -\mathbf{Q}_1\mathbf{C}_h & -\mathbf{Q}_2\mathbf{C} \\ -\mathbf{M}_1\mathbf{C}_h & -\mathbf{M}_2\mathbf{C} & -\mathbf{M}_1\mathbf{S}_h & -\mathbf{M}_2\mathbf{S} \end{bmatrix}\begin{bmatrix} \mathbf{E}_1 & \mathbf{E}_2 & \mathbf{0} & \mathbf{0} \\ \mathbf{0} & \mathbf{0} & \mathbf{E}_1\mathbf{R}_1 & \mathbf{E}_2\mathbf{R}_2 \\ \mathbf{E}_1\mathbf{C}_h & \mathbf{E}_2\mathbf{C} & \mathbf{E}_1\mathbf{S}_h & \mathbf{E}_2\mathbf{S} \\ \mathbf{E}_1\mathbf{R}_1\mathbf{S}_h & -\mathbf{E}_2\mathbf{R}_2\mathbf{S} & \mathbf{E}_1\mathbf{R}_1\mathbf{C}_h & \mathbf{E}_2\mathbf{R}_2\mathbf{C} \end{bmatrix}^{-1}\begin{bmatrix}\mathbf{d}_1\\ \mathbf{d}_2\end{bmatrix}$$

$$\text{or}\quad \mathbf{p}=\mathbf{kd} \tag{37}$$

The stiffness relationship of Eq. (37) is general and can be used in the normal way to assemble more complex forms. The required natural frequencies of the resulting structure are determined by evaluating its overall dynamic stiffness matrix at a trial frequency ω^* and using the Wittrick–Williams algorithm to establish how many natural frequencies have been exceeded by ω^*. This clearly provides the basis for a convergence procedure that can yield the required natural frequencies to any desired accuracy. The corresponding mode shapes can then be recovered by any appropriate method [21].

5. Wittrick–Williams algorithm

The Wittrick–Williams algorithm [22,23], for converging on the roots of transcendental eigenvalue problems, has been available for over 30 years and its use is widely understood. The algorithm is applied to the present problem in the form originally described by Howson and Williams [24], to which the reader is now directed. The reference shows that the key to converging on the required system frequencies lies in the calculation of two parameters, **B** and J_{ss}, for each member of the structure in turn. **B** is the dynamic stiffness matrix of a component member when the member is removed from the structure and then simply supported, while J_{ss} is the number of natural frequencies of this simply supported member that have been exceeded by the trial frequency.

Simply supported boundary conditions for the member are defined as follows:

$$\text{at } \xi=0 \text{ and } \xi=1,\quad U=V=\Phi=0,\quad \text{and}\quad M_x=M_y=B=0 \tag{38}$$

B can then be obtained by deleting appropriate rows and columns from Eq. (37).

The evaluation of J_{ss} is as follows. Examination of the boundary conditions in Eq. (38) show that they are satisfied by assuming solutions for the displacements $U(\xi)$, $V(\xi)$ and $\Phi(\xi)$ of the form

$$U(\xi) = C_i \sin(i\pi\xi), \quad V(\xi) = D_i \sin(i\pi\xi) \quad \text{and} \quad \Phi(\xi) = E_i \sin(i\pi\xi) \quad (i = 1, 2, 3, \ldots) \tag{39a–c}$$

where C_i, D_i and E_i are constants.

Substituting Eqs. (39) into Eq. (18) and noting that the non-trivial solutions correspond to those values of ω, the coupled natural frequencies of the member with simply supported ends, for which the determinant of the matrix is zero. i.e. when

$$\begin{vmatrix} (i\pi)^4 + \alpha_x^2(i\pi)^2 - \omega^2\beta_x^2 & 0 & -y_s\alpha_x^2(i\pi)^2 + y_c\omega^2\beta_x^2 \\ 0 & (i\pi)^4 + \alpha_y^2(i\pi)^2 - \omega^2\beta_y^2 & x_s\alpha_y^2(i\pi)^2 - x_c\omega^2\beta_y^2 \\ -y_s\dfrac{\alpha_x^2}{\gamma_x^2}(i\pi)^2 + y_c\omega^2\dfrac{\beta_x^2}{\gamma_x^2} & x_s\dfrac{\alpha_y^2}{\gamma_y^2}(i\pi)^2 - x_c\omega^2\dfrac{\beta_y^2}{\gamma_y^2} & (i\pi)^4 + \alpha_\varphi^2(i\pi)^2 - \omega^2\beta_\varphi^2 \end{vmatrix} = 0 \tag{40}$$

Eq. (40) is a cubic equation in ω^2 and yields three positive values of ω for each value of i. It is then possible to calculate J_{ss} by substituting progressively larger values of i until all of those natural frequencies lying below the trial frequency have been accounted for.

6. Examples

The work of this section consolidates the foregoing theory by performing a parametric study on a series of wall–frame structures of varying height using the proposed method and comparing their lower natural frequencies with datum values obtained from a fully converged finite element analysis of the original structures. The programme used to accomplish the latter was ETABS [25], in which the inter-storey member mass was lumped at each storey level using the automatic idealisation process.

Twelve asymmetric wall–frame structures are considered in all. They are catagorised into three groups according to their floor plan. These are shown in Figs. 7a–c and include the detailed arrangment of walls and frames that are all connected to each other by rigid diaphragms at each floor level. Each floor plan provides the footprint for a 10, 20, 40 and 60 storey asymmetric wall–frame structure, each with equal storey heights of 3 m throughout. It is clear that all the structures thus analysed comprise three walls and five plane frames running in the y direction and three walls and four plane frames running in the x direction. It should also be noted that the three floor plans have been chosen specifically to vary the proximity of O, S and C, the rigidity centre, the shear centre and the mass centre, respectively.

A concise description of the data for each of the twelve original frames and their equivalents in the proposed method is achieved using the idea of data groups. The relationship between the structures and their data groups is laid out in Table 1. Thus the first two columns of Table 1 define the building height and those storeys that have the same properties and hence the same data group. The next two columns define the corresponding data groups for Floor Plan 1. The first of these defines the data group for the original structure, while the second defines the data groups that together contain the data necessary for the proposed model. The corresponding data groups for Floor Plans 2 and 3 repeat across the table.

For simplicity in determining the nodal masses, half the mass of the walls and columns framing into and emanating from a floor diaphragm, together with the mass of the diaphragm and any associated beams, is stated as an equivalent uniformly distributed floor mass at that storey level. For all the examples presented, this value is arbitrarily taken to be $360\,\mathrm{kg/m^2}$ at each floor level, even where the stiffness properties of the inter-storey members change. Thus the centre of mass is at the geometric centre of the floor plan. This corresponds precisely to the automatic idealisation process in ETABS [25]. Finally the value of Young's modulus for all members is taken to be $E = 2 \times 10^{10}\,\mathrm{N/m^2}$. The data for the finite element models of the original structures can now be deduced from Tables 1 and 2. However, the data for the proposed method still requires further clarification.

In the 10 and 20 storey buildings, the properties of the structural elements do not change along the height of the structure, so each structure can be modelled using a single substitute beam element. In the 40 and 60 storey

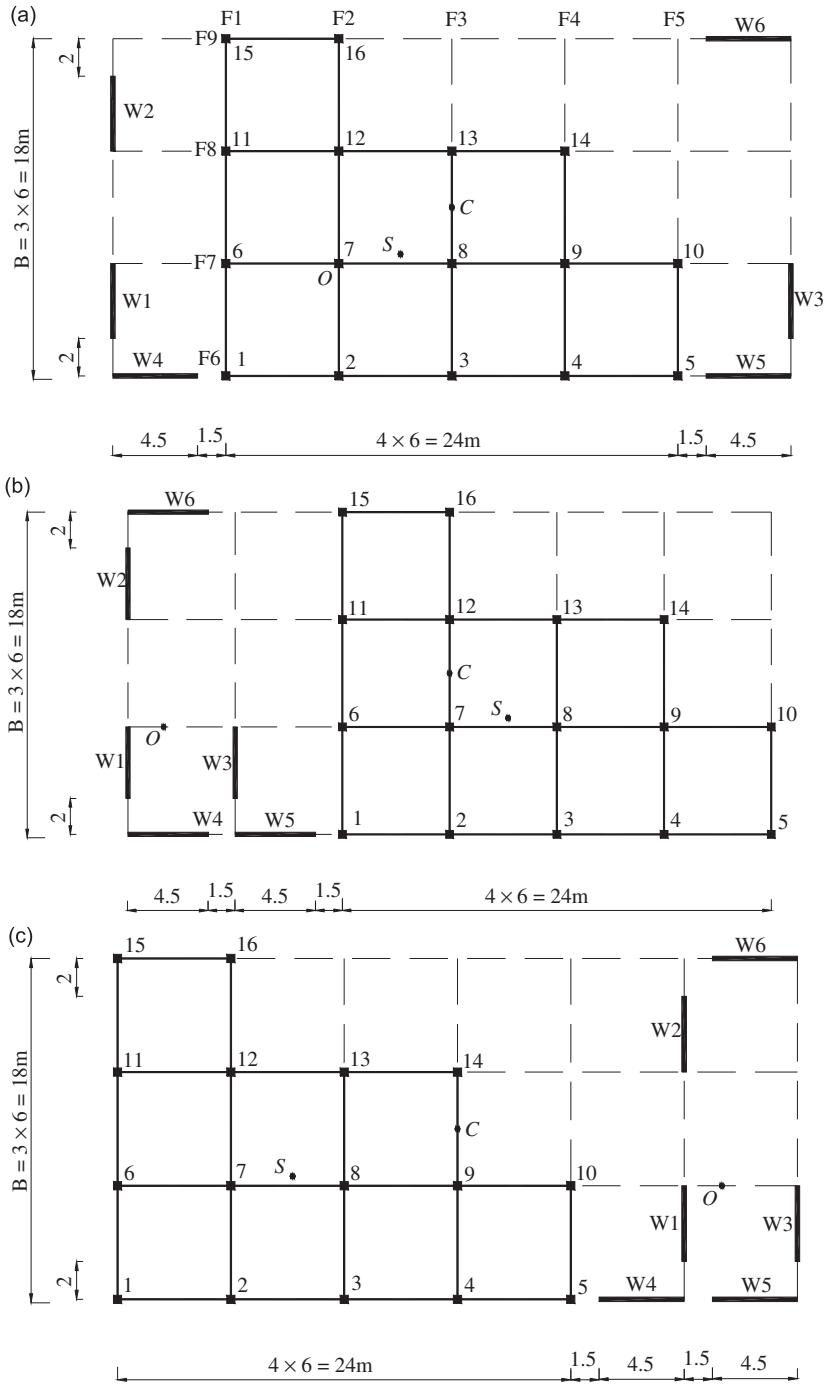

Fig. 7. (a) Floor Plan 1, (b) Floor Plan 2, (c) Floor Plan 3; for the family of 10, 20, 40 and 60 storey wall–frame structures of the Examples section. All dimensions are in metres.

buildings, the properties of the structural elements change in a stepwise fashion every 20 storeys. Thus they can be modelled with two and three substitute beam elements, respectively. The distributed mass of the substitute beams can be determined easily by smearing the total nodal mass of the original structure along the beam(s).

Table 1
The relationship between the original structures, the proposed models and their data groups

Building height (storeys)	Floors	Data group(s) required to define structure properties					
		Floor Plan 1		Floor Plan 2		Floor Plan 3	
		Original structure	Proposed model	Original structure	Proposed model	Original structure	Proposed model
10	1st to 10th	S1	A1 + B1 + C1	S1	A2 + B1 + C2	S1	A3 + B1 + C3
20	1st to 20th	S1	A1 + B1 + C1	S1	A2 + B1 + C2	S1	A3 + B1 + C3
40	1st to 20th	S2	A1 + B2 + C4	S2	A2 + B2 + C5	S2	A3 + B2 + C6
	21st to 40th	S1	A1 + B1 + C1	S1	A2 + B1 + C2	S1	A3 + B1 + C3
60	1st to 20th	S3	A1 + B3 + C7	S3	A2 + B3 + C8	S3	A3 + B3 + C9
	21st to 40th	S2	A1 + B2 + C4	S2	A2 + B2 + C5	S2	A3 + B2 + C6
	41st to 60th	S1	A1 + B1 + C1	S1	A2 + B1 + C2	S1	A3 + B1 + C3

Table 2
Member properties for each data group of the original structures

Data group	Properties	Columns (numbers are defined in Figs. 7a–7c)				Second moment of area of all beams (m^4)	Thickness of all walls (m)
		1,5,10, 14, 15,16	2,3,4,13	6,11	7,8,9,12		
S1	$I_x(m^4)$	0.005	0.005	0.01	0.01	0.00429	0.20
	$I_y(m^4)$	0.005	0.01	0.005	0.01		
S2	$I_x(m^4)$	0.01	0.01	0.02	0.02	0.00857	0.25
	$I_y(m^4)$	0.01	0.02	0.01	0.02		
S3	$I_x(m^4)$	0.02	0.02	0.04	0.04	0.01714	0.30
	$I_y(m^4)$	0.02	0.04	0.02	0.04		

I_x and I_y are the second moments of area of columns about the global x and y axes of Figs. 7a–c, respectively.
Young's modulus for all members is taken to be $E = 2 \times 10^{10}\,N/m^2$ and the effective mass at each floor level is $360\,kg/m^2$.

Table 3
Member properties of data groups A for the proposed model of each building

Data group	Properties					
	x_s (m)	y_s (m)	x_c (m)	y_c (m)	m (kg/m)	r_m^2 (m^2)
A1	3.273	0.500	6.000	3.000	77760	180
A2	19.273	0.500	16.000	3.000	77760	400
A3	−22.727	0.500	−14.000	3.000	77760	340

All the walls and frames in these examples are proportional, so that the flexure and shear centres at each floor level lie on vertical lines through the building. Hence the required eccentricities for Floor Plans 1, 2 and 3 in the x and y directions, the distributed mass of the substitute beam (smeared from the diaphragms) and the polar mass radius of gyration of the diaphragms about the flexure centre can then be calculated using the methods of Ref. [26] and then assembled into the data groups A of Table 3. The rigidities of the substitute beam(s) that are required for the proposed method may be calculated in the usual fashion and are presented as data groups B and C in Tables 4 and 5, respectively.

Table 4
Member properties of data groups B for the proposed model of each building

Data group	Properties			
	GA_x ($N \times 10^8$)	EI_x ($N\,m^2 \times 10^{10}$)	GA_y ($N \times 10^8$)	EI_y ($N\,m^2 \times 10^{10}$)
B1	5.647	9.113	5.176	6.400
B2	11.290	11.390	10.350	8.000
B3	22.590	13.670	20.710	9.600

Table 5
Member properties of data groups C for the proposed model of each building

Data group	Properties	
	GJ ($N\,m^2 \times 10^{11}$)	EI_w ($N\,m^4 \times 10^{12}$)
C1	0.5591	24.99
C2	2.426	7.073
C3	3.177	7.073
C4	1.118	31.24
C5	4.853	8.841
C6	6.355	8.841
C7	2.236	37.49
C8	9.705	10.61
C9	12.71	10.61

Table 6
Coupled natural frequencies (Hz) of the (a) 10-storey wall–frame buildings, (b) 20-storey wall–frame buildings, (c) 40-storey wall–frame buildings and (d) 60-storey wall–frame buildings with Floor Plans 1, 2 and 3 obtained from the continuum and FEM models

Freq. no.	Floor Plan 1			Floor Plan 2			Floor Plan 3		
	Proposed model	ETABS (FEM)	Diff. (%)	Proposed model	ETABS (FEM)	Diff. (%)	Proposed model	ETABS (FEM)	Diff. (%)
(a) 10-storey wall–frame buildings									
1	0.9377	0.8703	7.74	0.8875	0.8403	5.62	0.9756	0.9091	7.31
2	1.1085	1.0283	7.80	1.0908	1.0086	8.15	1.0587	0.9861	7.36
3	1.4082	1.2981	8.48	1.3505	1.2421	8.73	1.3452	1.2499	7.62
Av.			8.01			7.50			7.43
(b) 20-storey wall–frame buildings									
1	0.3664	0.3554	3.10	0.3899	0.3832	1.75	0.3475	0.3346	3.86
2	0.4377	0.4292	1.98	0.4065	0.3947	2.99	0.4415	0.4292	2.87
3	0.5259	0.5086	3.40	0.5013	0.4850	3.36	0.5457	0.5317	2.63
Av.			2.83			2.70			3.12
(c) 40-storey wall–frame buildings									
1	0.1914	0.1890	1.27	0.1966	0.1937	1.50	0.1627	0.1603	1.50
2	0.2439	0.2410	1.20	0.2385	0.2361	1.02	0.2481	0.2454	1.10
3	0.2767	0.2737	1.10	0.2719	0.2692	1.00	0.3216	0.3188	0.88
Av.			1.19			1.17			1.16
(d) 60-storey wall–frame buildings									
1	0.1485	0.1471	0.95	0.1487	0.1473	0.95	0.1212	0.1201	0.92
2	0.1937	0.1922	0.78	0.1923	0.191	0.68	0.1971	0.1959	0.61
3	0.2166	0.2158	0.37	0.2162	0.2154	0.37	0.2607	0.2595	0.46
Av.			0.70			0.67			0.66

7. Numerical results

Column 2, 5 and 8 of Tables 6a–d show the coupled natural frequencies (Hz) of the 10, 20, 40 and 60 storey wall–frame structures with Floor Plans 1, 2 and 3 obtained from the proposed three-dimensional shear–flexure–torsion beam theory, respectively. The third, sixth and ninth columns in each table show the results of a full finite element analysis of the corresponding original wall–frame structures. These results were obtained using the vibration programme ETABS in which the automatic idealisation process was utilised that assumes uniformly distributed mass on rigid floor diaphragms. Relevant comparisons are made in columns 4, 7 and 10.

8. Discussion

The proposed model has been developed in order to provide a simpler means of obtaining realistic approximations to the lower natural frequencies of complex multi-storey structures. The accuracy of the results for a range of typical structures compares well with those of a full finite element analysis, despite the fact that each model is very different. The most important features to note in the proposed model that distinguishes it from the finite element model can be summarised as follows:

- The original three-dimensional structure, which exhibits relatively complex interaction between its structural elements, can usually be modelled by a small number of simple substitute beams with few member properties.
- In the framed part of the original structure, the local bending rigidity of the individual columns and global bending deformation, due to the extensibility of the columns, have been neglected.
- There are no lumped masses in the proposed model in order to reduce the size of the problem (although this could easily be remedied). Thus the mass distribution of the original structure lies somewhere between the uniform mass distribution of the model and the lumped mass approximation of the finite element technique.

The simplifications mentioned above affect the results in differing proportions, depending upon the properties of the elements, geometry and the ratio of the rigidity of the frames to the rigidity of the walls in the original structure. In addition, some simplifications tend to increase the rigidity of the model while others reduce it. The influence of each factor on the accuracy of the proposed model still requires a more comprehensive investigation. However, the results in Tables 6b–d and Fig. 8 show that as the number of storeys increases, the difference between the results becomes significantly less. This stems mainly from the fact that the assumed mass distribution in the proposed and finite element models converge ever more closely as the number of storeys increases. Nevertheless, the difference between the model results and those of the finite element analysis still lie below 8% for all floor plans. More precisely, the results for the 20, 40 and 60 storey buildings would appear to be satisfactory since the difference between the model results and those of the finite

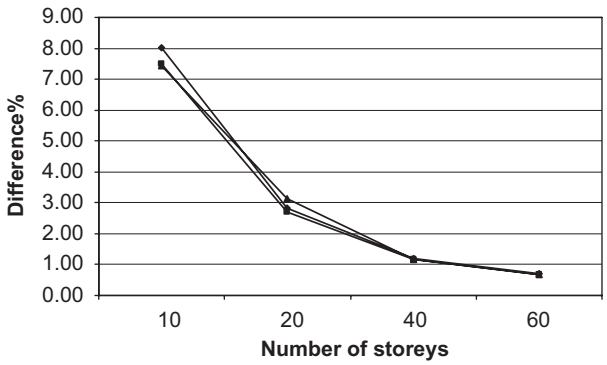

Fig. 8. Graphs of the difference between the averaged results from the proposed model and those from the full finite element analysis of the original structures for the three floor plans considered in the Examples section. –♦– Floor Plan 1 –■– Floor Plan 2 –▲– Floor Plan 3.

element analysis stays below 3% for all floor plans. Furthermore, comparison of the results in columns 4, 7 and 10 of Tables 6a–d and Fig. 8 indicates that the difference between the results of comparable structures with each of the floor plans is quite small. Although the proposed model has given satisfactory results for the 10–60 storey wall–frame structures tested, care should always be exercised when a relatively high degree of accuracy is desired. It is additionally recommended that further investigations are carried out on shorter and taller structures.

9. Conclusions

An approximate and relatively simple model has been developed for calculating the lower natural frequencies corresponding to overall modes of vibration of medium and tall building structures. Within this scope it can encompass many geometric configurations ranging from uniform structures with doubly symmetric floor plans to doubly asymmetric ones with step changes of member properties at any number of storey levels. The model has been developed on the assumption of uniformly distributed mass and stiffness and thus necessitates the solution of a transcendental eigenvalue problem. This can be solved to any desired accuracy by use of the Wittrick–Williams algorithm, which also guaranties that no natural frequencies can be missed. When all storeys of a frame can be considered to be identical, the required solutions can be found easily by hand. Results of a parametric study show that the model is likely to yield results of sufficient accuracy for engineering calculations when the number of storeys is greater than about ten and less than about sixty. As is inevitably the case when using simplified models, their accuracy should be thoroughly checked prior to use against datum results for the class of structure being considered.

References

[1] W.P. Howson, Global analysis: back to the future, *The Structural Engineer* 84 (3) (2006) 18–21.
[2] J.S. Kuang, S.C. Ng, Coupled lateral-torsion vibration of asymmetric shear-wall structures, *Thin-Walled Structures* 38 (2) (2000) 93–104.
[3] J.S. Kuang, S.C. Ng, Dynamic coupling of asymmetric shear wall structures: an analytical solution, *International Journal of Solids and Structures* 38 (48–49) (2001) 8723–8733.
[4] S.C. Ng, J.S. Kuang, Triply coupled vibration of asymmetric wall–frame structures, *Journal of Structural Engineering—ASCE* 126 (8) (2000) 982–987.
[5] J.S. Kuang, S.C. Ng, Coupled vibration of tall building structures, *Structural Design of Tall and Special Buildings* 13 (4) (2004) 291–303.
[6] Y. Wang, C. Arnaouti, S. Guo, A simple approximate formulation for the first two frequencies of asymmetric wall–frame multi-storey building structures, *Journal of Sound and Vibration* 236 (1) (2000) 141–160.
[7] K.A. Zalka, A simplified method for calculation of the natural frequencies of wall–frame buildings, *Engineering Structures* 23 (12) (2001) 1544–1555.
[8] K.A. Zalka, *Global Structural Analysis of Buildings*, E&FN Spon, London, 2001.
[9] G. Potzta, L.P. Kollar, Analysis of building structures by replacement sandwich beams, *International Journal of Solids and Structures* 40 (2003) 535–553.
[10] G. Tarjan, L.P. Kollar, Approximate analysis of building structures with identical stories subjected to earthquakes, *International Journal of Solids and Structures* 41 (2004) 1411–1433.
[11] S.K. Skattum, Dynamic analysis of coupled shear walls and sandwich beams, California Institute of Technology, Thesis, 1971.
[12] A.K. Basu, Seismic design charts for coupled shear walls, *Journal of Structural Engineering—ASCE* 109 (2) (1983) 335–352.
[13] R. Rosman, Stability and dynamics of shear wall frame structures, *Building Science* 9 (1974) 55–63.
[14] A. Rutenberg, Approximate natural frequencies for coupled shear walls, *Earthquake Engineering and Structural Dynamics* 4 (1975) 95–100.
[15] B.S. Smith, E. Crowe, Estimating periods of vibration of tall buildings, *Journal of Structural Engineering—ASCE* 112 (5) (1986) 1005–1019.
[16] B.S. Smith, Y.S. Yoon, Estimating seismic base shears of tall wall–frame buildings, *Journal of Structural Engineering—ASCE* 117 (10) (1991) 3026–3041.
[17] A. Kopecsiri, L.P. Kollar, Approximate seismic analysis of building structures by the continuum method, *Acta Technica Academiae Scientiarum Hungaricae* 108 (3–4) (1999) 417–446.
[18] A. Kopecsiri, L.P. Kollar, Simple formulas for the analysis of symmetric (plane) bracing structures subjected to earthquakes, *Acta Technica Academiae Scientiarum Hungaricae* 108 (3–4) (1999) 447–473.
[19] B. Rafezy, A. Zare, W.P. Howson, Coupled lateral-torsional frequencies of asymmetric, three-dimensional frame structures, *International Journal of Solids and Structures* 44 (2007) 128–144.

[20] B.S. Smith, A. Coull, *Tall Building Structures*, Wiley, New York, 1991.
[21] W.P. Howson, A compact method for computing the eigenvalues and eigenvectors of plane frames, *Advances in Engineering Software and Workstations* 1 (4) (1979) 181–190.
[22] F.W. Williams, W.H. Wittrick, An automatic computational procedure for calculating natural frequencies of skeletal structures, *International Journal of Mechanical Sciences* 12 (1970) 781–791.
[23] W.H. Wittrick, F.W. Williams, A general algorithm for computing natural frequencies of elastic structures, *The Quarterly Journal of Mechanics and Applied Mathematics* 24 (3) (1971) 263–284.
[24] W.P. Howson, F.W. Williams, Natural frequencies of frames with axially loaded Timoshenko members, *Journal of Sound and Vibration* 26 (4) (1973) 503–515.
[25] E.L. Wilson, J.P. Hollings, H.H. Dovey, ETABS version 6, Three-dimensional analysis of building structures, 1995.
[26] V.W.T. Cheung, W.K. Tso, Eccentricity in irregular multi-storey buildings, *Canadian Journal of Civil Engineering* 13 (1) (1986) 46–52.